Journal of Coastal and Marine Engineering
Volume 1 • Number 1 • June 2018

Pipeline Route Selection Effects on Seawater Intakes Efficiency (Case Study: Bandar Abbas Sako Desalination Plant)

Seyede Masoome Sadaghi[1*], Ali Fakher[2], Zeinab Toorang[3] and Alireza Shafieefar[4]

1) Road, Housing and Urban Development Research Center. Ministry of Road and Urban Development, Tehran, Iran, s.sadaghi@bhrc.ac.ir
2) School of Civil Engineering, University of Tehran, Tehran, Iran, afakher@ut.ac.ir
3) Pars Geometry Consultants, Tehran, Iran, z.toorang@parsgc.com
4) Pars Geometry Consultants, Tehran, Iran, a.shafieefar@parsgc.com

Abstract: In the present paper, Bandar Abbas SAKO desalination plant is considered as a case study and the seawater intake and outfall system is investigated from the viewpoint of route optimization. MIKE21-FM and MIKE3-FM have been used for hydrodynamic and salinity dispersion numerical modeling. Intake water quality, recirculation and environmental consideration were the key factors considered in the route optimization. It has been shown that the selection of the right route for the intake and discharge pipelines has a significant effect on the whole system efficiency.

Keywords: Seawater Intake; Submarine Pipelines; Route Selection; Salinity Dispersion

1. Introduction

Seawater is an important source of water for the consumption of power plants, refineries and desalination plants. Water scarcity and the necessity of supplying a portion of water demand from sea, has led to an increase in the need for seawater intakes. It has been suggested that seawater when used as feed water especially for desalination facilities, improves with depth due to lower primary productivity caused by light absorbance and a lower concentration of suspended sediment in the water column [1, 2]. Deep ocean intakes will produce a higher quality feed water based on some oceanographic investigations at various locations [3, 4, 5, 6].

Construction of onshore intake basins and supply of water via submarine pipelines is a common method which has been used in many projects to provide high quality water from deeper parts of seas and oceans. The intake and discharge pipeline routes are designed to reach the required water quality without recirculation. The environmental criteria shall also be met in selecting the outfall point [7].

2. Project Explanation

Bandar Abbas SAKO desalination plant is one of the world's largest integrated water and power plants. The desalination final production capacity will reach one million cubic meters per day (CMD). The feed water for desalination and power plant cooling system will be supplied from sea by means of a seawater intake system based on a gravity filled basin. With total capacity of four million CMD, this intake will be the biggest desalination plant in the world. The plant is under construction at west of ISOICO shipyard. The project location is shown in Figures 1 and 2 [8].

Figure 1. Project location

Figure 2. Project location at west of ISOICO shipyard

In the basic design, six intake pipelines (HDPE, D_{in}=2.5 m) perpendicular to the intake basin structure, were supposed to supply seawater with the desired quality,

*Corresponding author

from the distance of about 3.1 km offshore (depth of -12 m. CD along route 1). Due to the long length of the pipelines, the second alternative as shown in Figure 3 was proposed for the intake route. More investigations revealed a deep area in the vicinity of the project. The third route alternative is considered to reach the mentioned area.

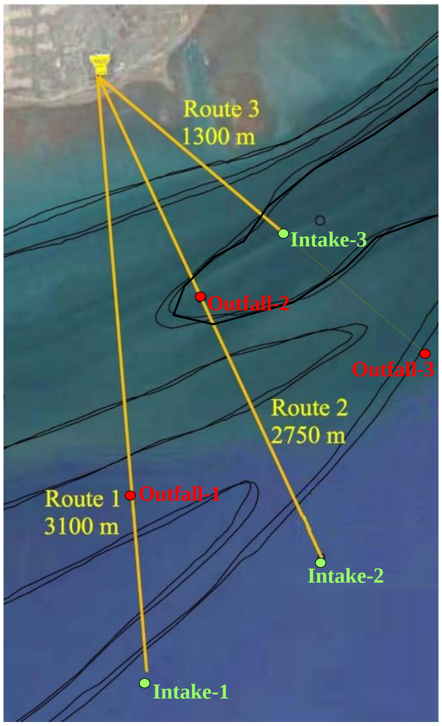

Figure 3. Pipeline route alternatives

The pipe length for each alternative is presented in Table 1.

Table 1. Pipe lengths in different alternatives

Alt.	Intake pipe length (m)	Outfall pipe length (m)	Total pipe length (m)
1	6×3100=18600	3×2250=6750	25350
2	6×2750=16500	3×1300=3900	20400
3	6×1300=7800	3×2100=6300	14100

Discharging saline water from desalination system and heated water from the cooling system of the power plant into the sea may result in two major problems namely environmental pollutions and saline water recirculation. These items shall be considered in the selection of discharge point. For selection of intake and discharge points, the following items were investigated in each alternative.

2.1. Intake Water Quality

It is assumed that the water quality improves with depth. Initial investigations had shown that the water quality at the depth of 12 m CD in front of the basin meets the minimum requirements for the desalination feed water. For new alternatives, it was assumed that the water quality at the same depth has the required quality. Further water quality tests were conducted to confirm these assumptions. The results proved that there was no significant difference in the water quality at the intake points of three mentioned routes [8].

2.2. Intake/Outfall Recirculation

In each alternative, the outfall shall be located in a point where the discharge flow cannot return to the intake line because recirculation can lead to progressive decrease in the efficiency of desalination system. In tide dominant regions where the current direction reverses, the outfall is usually located along the intake route so the tidal currents always conduct the brine stream away from the intake. The outfall is usually closer to the shoreline compared to the intake point. This common practice is proved to be possible for the first and second alternatives in SAKO project by mathematical modeling but for the third alternative, the distance between the intake and shoreline is not long enough to accommodate the discharge point. Hence the outfall pipeline is extended beyond the intake point to the depth where this criterion is met.

2.3. Environmental Considerations

Iran's Department of Environment has some regulations for brine or heated discharges. According to these regulations, the salinity increment at the distance of 200 m from outfall should not exceed 10% of the initial salinity [9]. The required dispersion and mixing is easier to be achieved in deeper waters. Hence, outfall lines usually extend toward deep waters until reaching a point where the environmental criterion is met. The discharge points in the mentioned alternatives are all checked by mathematical modeling to ensure that the environmental criterion is met.

3. Mathematical Modeling

In this study, dispersion simulation was performed by numerical modeling using MIKE21-FM and MIKE3-FM. These two models have been used for regional and local models, respectively. Results of regional model that is a two dimensional hydrodynamic model have been employed in the local salinity dispersion model as its boundary condition data.

3.1. Regional Model

MIKE-21 flow model has been used for numerical simulation of tidal current and water levels in large scale regional model for prediction of boundary conditions of local 3D model [10].

3.1.1. Model Description

The hydrodynamic module of MIKE-21-FM is based on the numerical solution of the two dimensional shallow water equations- the depth integrated incompressible Reynolds averaged Navier-Stokes equations. Thus, the model consists of continuity and momentum equations. The spatial discretization of the primitive equations is performed using a cell-centered finite volume method. In the horizontal plane, an unstructured grid consisting of triangle elements is used. For the time integration, an explicit scheme is used.

2D shallow water equations obtained by integration of the horizontal momentum equations and the continuity equation over depth $h = \eta + d$ are:

$$\frac{\partial h}{\partial t} + \frac{\partial h\bar{u}}{\partial x} + \frac{\partial h\bar{v}}{\partial y} = hS \tag{1}$$

$$\frac{\partial h\bar{u}}{\partial t} + \frac{\partial h\bar{u}^2}{\partial x} + \frac{\partial h\overline{vu}}{\partial y} = f\bar{v}h - gh\frac{\partial \eta}{\partial x} - \frac{h}{\rho_0}\frac{\partial p_a}{\partial x} - \frac{gh^2}{2\rho_0}\frac{\partial \rho}{\partial x} + \frac{\tau_{sx}}{\rho_0} - \frac{\tau_{bx}}{\rho_0} - \frac{1}{\rho_0}\left(\frac{\partial s_{xx}}{\partial x} + \frac{\partial s_{xy}}{\partial y}\right) + \frac{\partial}{\partial x}\left(hT_{xx}\right) + \frac{\partial}{\partial y}\left(hT_{xy}\right) + hu_sS \tag{2}$$

$$\frac{\partial h\bar{v}}{\partial t} + \frac{\partial h\overline{uv}}{\partial x} + \frac{\partial h\bar{v}^2}{\partial y} = -f\bar{u}h - gh\frac{\partial \eta}{\partial y} - \frac{h}{\rho_0}\frac{\partial p_a}{\partial y} - \frac{gh^2}{2\rho_0}\frac{\partial \rho}{\partial y} + \frac{\tau_{sy}}{\rho_0} - \frac{\tau_{by}}{\rho_0} - \frac{1}{\rho_0}\left(\frac{\partial s_{yx}}{\partial x} + \frac{\partial s_{yy}}{\partial y}\right) + \frac{\partial}{\partial x}\left(hT_{xy}\right) + \frac{\partial}{\partial y}\left(hT_{yy}\right) + hv_sS \tag{3}$$

The overbar indicates a depth average value. For example, $\bar{u}$ and $\bar{v}$ are the depth averaged velocities defined by

$$h\bar{u} = \int_{-d}^{\eta} u\,dz\ ,\ h\bar{v} = \int_{-d}^{\eta} v\,dz \tag{4}$$

The lateral stresses T_{ij} include viscous friction, turbulent friction and differential advection. They are estimated using an eddy viscosity formulation based on the depth average velocity gradients

$$T_{xx} = 2A\frac{\partial \bar{u}}{\partial x}\ ,\ T_{xy} = A\left(\frac{\partial \bar{u}}{\partial y} + \frac{\partial \bar{v}}{\partial x}\right)\ ,\ T_{yy} = 2A\frac{\partial \bar{v}}{\partial y} \tag{5}$$

In the above equations, t is the time, x, y and z are the Cartesian coordinates, η is the surface elevation, d is the still water depth, $h = \eta + d$ is the total water depth, u and v are the velocity components in the x and y directions. $f = 2\Omega\sin\phi$ is the Coriolis parameter (Ω is the angular rate of revolution and ϕ the geographic latitude), g is the gravitational acceleration, ρ is the density of water, s_{xx}, s_{xy}, s_{yx} and s_{yy} are components of the radiation stress, p_a is the atmospheric pressure, ρ_0 is the reference density of water, S is the magnitude of the discharge due to point sources and (u_s, v_s) is the velocity by which the water is discharged into the ambient water, A is the horizontal eddy viscosity, (τ_{sx}, τ_{sy}) and (τ_{bx}, τ_{by}) are the x and y components of the surface wind and bottom stresses [10].

3.1.2. Model Set-up

The regional model covers the entire Persian Gulf, the Strait of Hormuz and the inner part of Oman Sea. In computational domain, finer grids around the project area and coast line are utilized to obtain accurate results around the project area. Figure 4 shows the computational mesh of the simulation zone [11].

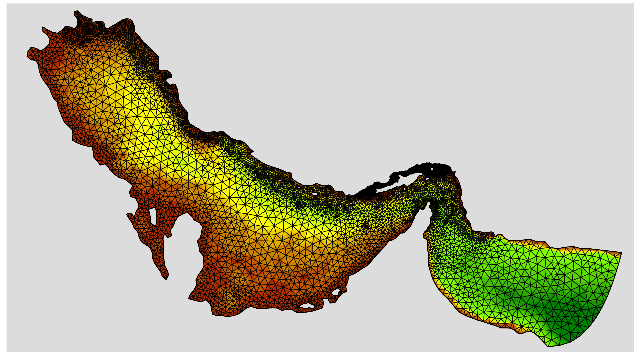

Figure 4- Regional model domain and its computational mesh

Flooding and drying and Coriolis effect have been taken into consideration in the model. Eddy viscosity is considered by Smagorinsky formulation. The default value for dimensionless coefficient of this formulation is 0.28. Manning formulation is chosen for bed resistance. The east side of the model area is considered as curved open boundary and tidal elevation time history which is predicted based on Chabahar station is considered for the boundary condition.

For model calibration, available ADCP which measured data for a duration of one month (22 Jun- 22 Jul) at two different locations have been utilized. The Manning number has been used as a calibration factor to achieve the best fit between measured and modeled data including surface elevation, current speed and direction. A sample comparison between surface elevation in measured and modeled data is shown in Figure 5.

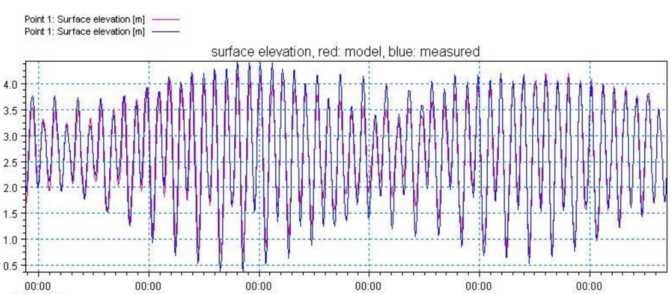

Figure 5- Measured and Modeled Surface Elevation Comparison (Jun- Jul)

3.2. Local Model

MIKE-3 FLOW MODEL FM, the most recent flow module of MIKE3, has been used for local simulation and analysis of salinity dispersion. Since flow velocity and water salinity in the vicinity of outfall do not have a homogeneous distribution in depth, 3D models should be applied. This model can be employed to simulate variations in surface elevation and current velocities in variety of cases; especially when there is current velocities variation in depth or when density stratification occurs [10].

3.2.1. Model Description

The model is based on the solution of the three-dimensional incompressible Reynolds averaged Navier-Stokes equations, subject to the assumptions of Boussinesq and hydrostatic pressure. The local continuity equation and the two horizontal momentum equations for the x- and y-components are presented herein:

$$\frac{\partial u}{\partial x}+\frac{\partial v}{\partial y}+\frac{\partial w}{\partial z}=S \tag{6}$$

$$\begin{aligned}&\frac{\partial u}{\partial t}+\frac{\partial u^2}{\partial x}+\frac{\partial vu}{\partial y}+\frac{\partial wu}{\partial z}= fv-g\frac{\partial \eta}{\partial x}-\frac{1}{\rho_0}\frac{\partial p_a}{\partial x}-\\&\frac{g}{\rho_0}\int_z^{\eta}\frac{\partial \rho}{\partial x}dz-\frac{1}{\rho_0 h}\left(\frac{\partial s_{xx}}{\partial x}+\frac{\partial s_{xy}}{\partial y}\right)+\\&F_u+\frac{\partial}{\partial z}\left(\nu_t\frac{\partial u}{\partial z}\right)+u_s S\end{aligned} \tag{7}$$

$$\begin{aligned}&\frac{\partial v}{\partial t}+\frac{\partial v^2}{\partial y}+\frac{\partial uv}{\partial x}+\frac{\partial wv}{\partial z}=-fu-g\frac{\partial \eta}{\partial y}-\frac{1}{\rho_0}\frac{\partial p_a}{\partial y}-\\&\frac{g}{\rho_0}\int_z^{\eta}\frac{\partial \rho}{\partial y}dz-\frac{1}{\rho_0 h}\left(\frac{\partial s_{yx}}{\partial x}+\frac{\partial s_{yy}}{\partial y}\right)+\\&F_v+\frac{\partial}{\partial z}\left(\nu_t\frac{\partial v}{\partial z}\right)+v_s S\end{aligned} \tag{8}$$

where, t is the time, x, y and z are the Cartesian coordinates, η is the surface elevation, d is the still water depth, $h=\eta+d$ is the total water depth, u, v and w are the velocity components in the x, y and z directions. $f=2\Omega\sin\phi$ is the Coriolis parameter (Ω is the angular rate of revolution and ϕ the geographic latitude), g is the gravitational acceleration, ρ is the density of water, s_{xx}, s_{xy}, s_{yx} and s_{yy} are components of the radiation stress, p_a is the atmospheric pressure, ρ_0 is the reference density of water, S is the magnitude of the discharge due to point sources and (u_s, v_s) is the velocity by which the water is discharged into the ambient water, A is the horizontal eddy viscosity, (τ_{sx}, τ_{sy}) and (τ_{bx}, τ_{by}) are the x and y components of the surface wind and bottom stresses. The horizontal stress terms are described using a gradient-stress relation, which is simplified to

$$F_u=\frac{\partial}{\partial x}\left(2A\frac{\partial u}{\partial x}\right)+\frac{\partial}{\partial y}\left(A\left(\frac{\partial u}{\partial y}+\frac{\partial v}{\partial x}\right)\right) \tag{9}$$

$$F_v=\frac{\partial}{\partial x}\left(A\left(\frac{\partial u}{\partial y}+\frac{\partial v}{\partial x}\right)\right)+\frac{\partial}{\partial y}\left(2A\frac{\partial v}{\partial y}\right) \tag{10}$$

The transport of temperature, T, and salinity, s, follows the general transport-diffusion equation as

$$\begin{aligned}&\frac{\partial T}{\partial t}+\frac{\partial uT}{\partial x}+\frac{\partial vT}{\partial y}+\frac{\partial wT}{\partial z}=F_T+\\&\frac{\partial}{\partial z}\left(D_v\frac{\partial T}{\partial z}\right)+\hat{H}+T_s S\end{aligned} \tag{11}$$

$$\frac{\partial s}{\partial t}+\frac{\partial us}{\partial x}+\frac{\partial vs}{\partial y}+\frac{\partial ws}{\partial z}=F_s+\frac{\partial}{\partial z}\left(D_v\frac{\partial s}{\partial z}\right)+s_s S \tag{12}$$

Where D_v is the vertical turbulent (eddy) diffusion coefficient. $\hat{H}$ is a source term due to heat exchange with the atmosphere. T_s and s_s are the temperature and the salinity of the source. F are the horizontal diffusion terms defined by

$$\left(F_T, F_s\right)=\left[\frac{\partial}{\partial x}\left(D_h\frac{\partial}{\partial x}\right)+\frac{\partial}{\partial y}\left(D_h\frac{\partial}{\partial y}\right)\right](T, s) \tag{13}$$

Where D_h is the horizontal diffusion coefficient. The diffusion coefficients can be related to the eddy viscosity

$$D_h=\frac{A}{\sigma_T} \tag{14}$$

$$D_v=\frac{\nu_t}{\sigma_T} \tag{15}$$

Where σ_T is the Prandtl number. In many applications, a constant Prandtl number can be used [10].

3.2.2. Model Set-up

The computational domain of 3D model covers the entire northern area of Qeshm Island including Strait of Hormuz. The regional and local domains are shown in Figure 6. Designed mesh for the local model is presented in Figure 7. Finer grids in particular areas such as shallow water and nearshore and especially around the outfall and intake locations have been used to obtain accurate results. Four equidistance vertical layers have been considered for vertical discretization throughout the computational domain. The modeling area includes two open wet boundaries on the west and east for which salinity and hydrodynamic boundary conditions were defined. Hydrodynamic boundary data were extracted from the 2D regional model in the form of spatially and temporally variable data sets. Based on the salinity of Persian Gulf around the project area, the salinity value for initial condition as well as for all boundaries has been assigned to be 37.5 PSU [11].

4. Route Optimization

Considering the above explanations, different numerical models were designed to check the recirculation and environmental criteria for different possible alternatives [11]. Based on environmental criteria, salinity increment at the distance of 200 m from outfall should not exceed 10% of initial salinity. Therefore, some points around the different assumed outfalls at the distance of 200 m are selected for checking the environmental criterion.

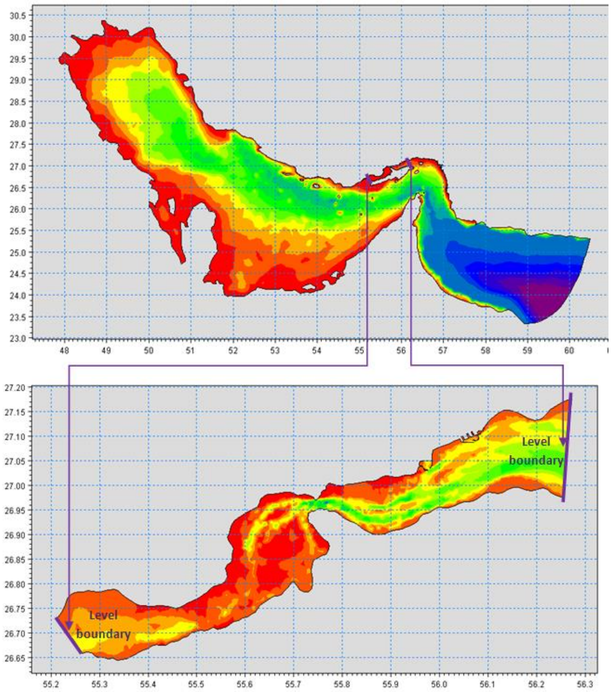

Figure 6. Regional and local model domains

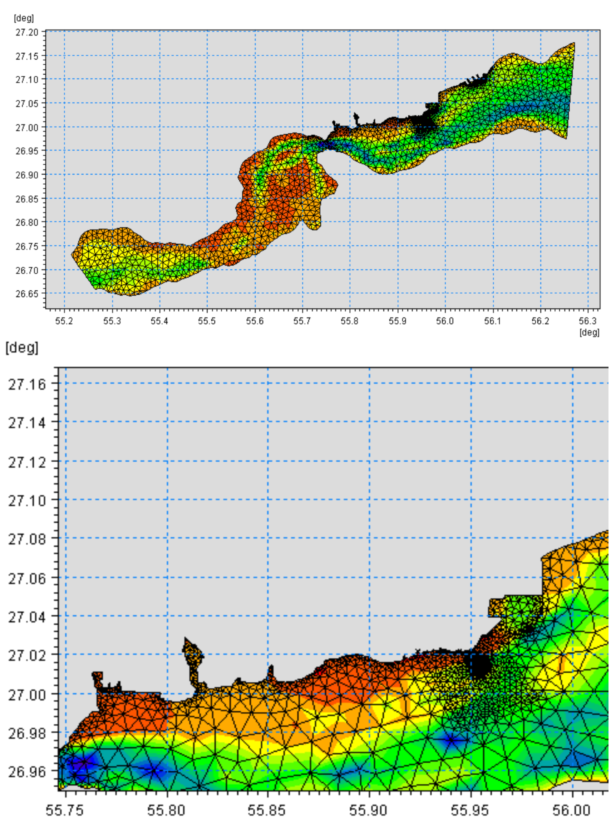

Figure 7. Mesh generated for 3D local model

In addition, the salinity increment in the intake point should be negligible. It means that, intake water should not be affected by salinity plume of outfall. For this purpose, the salinity increment values at the intake points are extracted and presented as time series charts. A sample dispersion pattern for the 3rd alternative is shown in Figure 8 [10, 11].

According to the results, the third alternative was proved to fulfill both recirculation and environmental criteria. In this innovative approach, unlike the common practice, the intake is located closer to the shoreline in comparison with the outfall point.

A sample of salinity increment time series at intake point of the third alternative for surface and near bed locations are shown in Figure 9.

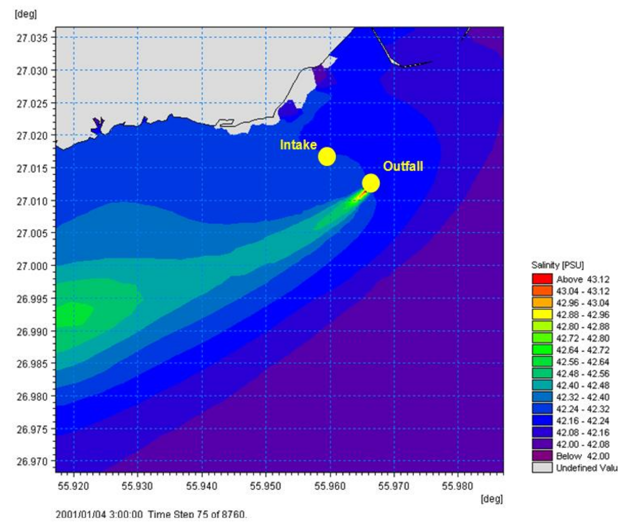

Figure 8. Salinity dispersion pattern for the 3rd alternative

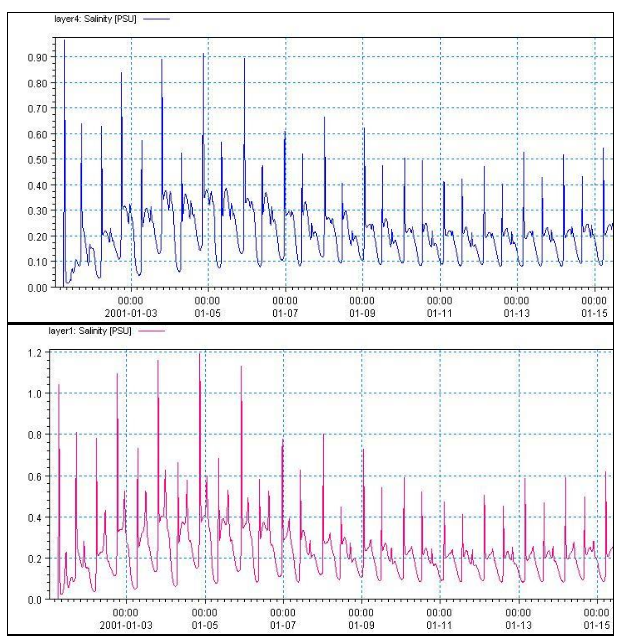

Figure 9. Salinity increment in surface (top) and near bed (bottom) at the intake location- alternative 3

The selected alternatives are also evaluated from an economical perspective. The construction costs of these alternatives are compared to each other to select the most optimized route for the pipelines. Cost estimations are roughly measured by taking into consideration only the major effective parameters. These parameters include the costs of procurement and installation of pipelines, dredging and backfilling operations. Unit costs for the effective parameters are assumed based on local experiences, in order to achieve a rational comparison between the alternatives.

Considering all the above mentioned aspects, the third alternative is concluded to be the most optimized choice. The most notable advantages of this alternative are summarized below:

– Due to the considerable decrease in pipes length (decrease of about 11250 m HDPE pipes) and associated dredging volumes, the construction costs attributed to the optimized route were decreased more than 25% compared to the initial plan.

– The operation and maintenance costs of the third alternative are much less than the existing plan due to a major reduction in the total pipeline lengths.

– The reduction of intake pipes length decreases the linear head losses considerably which increases the hydraulic capacity of pipes and the intake basin.

– The increase in the intake capacity in the third alternative leads to higher system availability and reliability especially for extreme conditions.

5. Conclusion

The present study has shown that the route selection for submarine pipelines in seawater intake and outfall systems, has considerable effects on project overall costs and efficiency. In route selection, different aspects should be considered simultaneously. In most cases, the shortest route perpendicular to the coastline is selected for the pipeline route, but the present study has shown that more investigation about the optimized route may lead to considerable improvements in project overall efficiency and cost benefits. The shortest routes eventuate the lowest costs but it should be proved to fulfill the required intake water quality and avoid the recirculation between intake and outfall. The environmental criteria should also be met around outfall point. Numerical models are of great use in selecting the best route which fulfills all the desired criteria.

6. References

[1]. Gille, D. “Seawater intakes for desalination plants”, Desalination, 156(1–3), 249–256, 2003.

[2]. Cartier, G, & Corsin, P. “Description of different water intakes for SWRO plants”. In Proceedings of the International Desalination Association World Congress on Desalination and Water Reuse, Gran Canaria, Spain, October 21–26, 2007, Paper IDAWC/MP07-185.

[3]. Hayashi, M., Ikeda, T., Otsuka, K., & Takahashi, M. M. “Assessment on environmental effects of deep ocean water discharged into coastal sea”. In: Saxena, N. (ed.) Marine Science and Technology, PACON International, 535–546, 2003.

[4]. Takahashi, M., & Ikeya, T. “Ocean fertilization using deep ocean water (DOW)”. Deep Ocean Water Research, 4, 73–87, 2003.

[5]. Takahashi, M., & Yamashita, K. “Clean and safe supply of fish and shellfish to clear the HACCP regulation by use of clean and cold water in Rausu, Hokkaido, Japan”. Japan Journal of Oceanography, 4, 219–223, 2005.

[6]. Takahashi, M., & Huang, P.-Y. “Novel renewable natural resource of deep ocean water (DOW) and their current and future practical applications”. Kuroshio Science, 6, 101–113, 2012.

[7]. Pankratz, T., “An Overview of Seawater Intake Facilities for Seawater Desalination”. CH2M Hill, Inc.

[8]. Pars Geometry Consultants, SAKO Desalination Plant, “Design general data” report, 2015.

[9]. Iranian Environmental Protection Organization Standard for effluent disposal, Department of Environment of Iran

[10]. Mike 21 User Manual, Danish Hydraulic Engineering (DHI), Denmark, 2014

[11]. Pars Geometry Consultants, SAKO Desalination Plant, “Evaluation of salinity distribution and saline water recirculation” report, 2015.